International Journal of Astrobiology 15 (3): 231–238 (2016)
doi:10.1017/S1473550415000439 © Cambridge University Press 2015

Carbonization in Titan Tholins: implication for low albedo on surfaces of Centaurs and trans-Neptunian objects

Chaitanya Giri[1,2], Christopher P. McKay[3], Fred Goesmann[1], Nadine Schäfer[4], Xiang Li[5], Harald Steininger[1], William B. Brinckerhoff[6], Thomas Gautier[1,6], Joachim Reitner[4,7] and Uwe J. Meierhenrich[2]

[1]*Max Planck Institute for Solar System Research, Justus-von-Liebig-Weg 3, 37077 Göttingen, Germany*
e-mail: giri@mps.mpg.de
[2]*Institut de Chimie de Nice, University of Nice Sophia Antipolis, CNRS UMR 7272, 28 Avenue Valrose, 06108 Nice Cedex 2, France*
[3]*Space Science Division, NASA Ames Research Center, Moffett Field, CA 94035, USA*
[4]*Geoscience Centre, Department of Geobiology, Georg-August-Universität Göttingen, Goldschmidtstraße 3, 37077 Göttingen, Germany*
[5]*Center for Research and Exploration in Space Science & Technology, University of Maryland, Baltimore County, Baltimore, MD 21250, USA*
[6]*NASA Goddard Space Flight Center, Greenbelt, MD 20771, USA*
[7]*Göttingen Academy of Sciences and Humanities, Theaterstraße 7, 37073 Göttingen, Germany*

Abstract: Astronomical observations of Centaurs and trans-Neptunian objects (TNOs) yield two characteristic features – near-infrared (NIR) reflectance and low geometric albedo. The first feature apparently originates due to complex organic material on their surfaces, but the origin of the material contributing to low albedo is not well understood. Titan tholins synthesized to simulate aerosols in the atmosphere of Saturn's moon Titan have also been used for simulating the NIR reflectances of several Centaurs and TNOs. Here, we report novel detections of large polycyclic aromatic hydrocarbons, nanoscopic soot aggregates and cauliflower-like graphite within Titan tholins. We put forth a proof of concept stating the surfaces of Centaurs and TNOs may perhaps comprise of highly 'carbonized' complex organic material, analogous to the tholins we investigated. Such material would apparently be capable of contributing to the NIR reflectances and to the low geometric albedos simultaneously.

Received 5 October 2015, accepted 6 October 2015, first published online 28 December 2015

Key words: albedo, Centaur, graphite, organics, PAH, soot, Titan, tholins, trans-Neptunian objects.

Introduction

Astronomical studies have shown several small bodies, presently located in or originating from the outer Solar System, having surfaces covered with material of extremely low geometric albedo that is either neutral (black) or dark red in colour (Cruikshank 1987). Two independent analyses from the earliest of such research initiatives, one using pyrolysis–gas chromatography–mass spectrometry (Py–GC–MS) on a fallen Orgueil (C1) chondrite (Bandurski & Nagy 1976) and a second investigating astronomical reflectance spectra of the Centaur 944 Hidalgo (Gradie & Veverka 1980), proposed the possible presence of complex organic material akin to terrestrial kerogen, although of non-biogenic origin, on the surfaces of small Solar System objects. These observations were supported by the argument that complex organic solids could not only be synthesized on inner Solar System asteroids by Fischer–Tropsch-like reactions (Hayatsu *et al.* 1971; Studier *et al.* 1972; Hayatsu & Anders 1981), but also on interstellar grain surfaces (Sagan & Khare 1979). Overall the research carried out to date, in forms of laboratory simulations, astronomical observations and analyses of extraterrestrial material therefore, indicate that complex organics could possibly be the reservoirs of prebiotic species and they could be abundant throughout the Solar System (Kerridge 1999; Kwok 2009).

The term 'tholins' refers to a wide class of brownish–blackish highly viscous organic residues formed from irradiation of cosmically relevant gases (Sagan & Khare 1979; Cable *et al.* 2011). Tholins are synthesized with several gaseous precursors and under varied experimental conditions. These diverse materials and conditions generate distinct organic residues but with certain overarching properties. Such distinct tholins simulate macromolecular organic material on Saturn's moon Titan, icy moons such as Triton, primitive Earth, and Centaurs, comets and trans-Neptunian objects (TNOs). Tholins synthesized by tesla coil electrical discharge under conditions that simulate the N_2 and methane (CH_4) dominant atmosphere of Titan (Khare *et al.* 1984) have been a common ingredient of mixtures, used to fit the astronomical near-infrared (NIR) reflectances of Centaurs and TNOs. Centaurs whose astronomical NIR spectra are modelled with mixtures containing Titan tholins include 5145 Pholus (Cruikshank *et al.* 1998), 10199 Chariklo (Dotto *et al.* 2003a), 52872 Okyrhoe (DeMeo *et al.*

https://doi.org/10.1017/S1473550415000439 Published online by Cambridge University Press

2010), 8405 Asbolus (Barucci *et al.* 2000), (55576) 2002 GB_{10} and (83982) 2002 GO_9 (Dorresoundiram *et al.* 2005), and the TNOs include 90482 Orcus, (73480) 2002 PN_{34}* (DeMeo *et al.* 2010), (47171) 1999 TC36 (Dotto *et al.* 2003b) and (55565) 2002 AW_{197} (Dorresoundiram *et al.* 2005).

Despite the essentiality of Titan tholins in simulation mixtures, their laboratory synthesis conditions do not represent the environment on Centaurs and TNOs, particularly the volatile precursors, their compositions, temperature, pressure and radiation flux regimes. Scattered attempts to synthesize tholins approximately representing the organic material on icy Solar System bodies have been undertaken. These tholins were designated differently as Triton or ice tholins (Khare *et al.* 1989, 1993; McDonald *et al.* 1994, 1996); however, until now not much analytical progress has been made regarding these tholins. The single-most factor for this research limitation has been their low production amounts as compared with Titan tholins. Yet, along with Titan tholins, Triton tholins have also been a regular component in the geographical mixtures simulating the reflectance of several Centaurs and TNOs.

The motivation of our investigation is to comprehend the chemical composition of Titan tholins, especially the components that allow the spectral matching of Centaurs and TNOs. This consistent use makes Titan tholins a plausible analogue to the surface chemical compositions of Centaurs and TNOs; however this plausibility demanded investigations beyond the NIR studies applied generally. We elucidate the material properties that contribute to the extremely low geometric albedo (0.05–0.15) by investigating the chemical structure and composition of Titan tholins using multiple analytical techniques such as Py–GC–MS, laser desorption–time-of-flight–mass spectrometry (LD–TOF–MS), Raman spectroscopy and field-emission scanning electron microscopy (FE-SEM).

Materials and methods

Production of tholins

The Titan tholins (hereafter 'tholins') used in this study were synthesized at the NASA Ames Research Center, USA. Following the description by McKay (1996), a gas mixture of 10% CH_4 in N_2 was introduced in a 3 litres glass reactor at a gas flow rate of ~ 3 cm^3 min^{-1}. The pressure within the reactor was maintained at slightly above ambient. Three sets of tungsten electrodes, each with an arc-gap of 0.5 cm, were inserted into the reactor. They were energized via electrical discharge from a tesla coil, where each coil was cyclically switched on for 15 min. The entire apparatus was operated for 3 weeks at ambient temperature, which eventually led to accumulation of tholins on the inner walls of the reactor. The accumulated tholins were scraped carefully and packed in air-tight vials.

The elemental composition of tholins produced in these simulations has been reported to be 67.2% C, 5.79% H, 14.2% N and 12% O (McKay 1996). Oxygen was not present in the initial gas mixture and is believed to be an oxidative contaminant present throughout the tholins chemical structure.

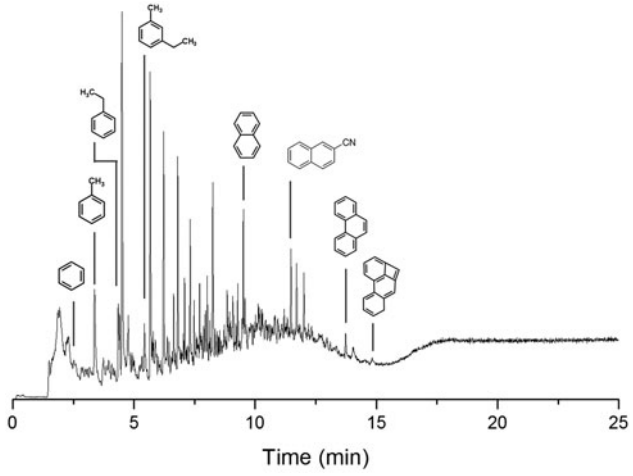


Fig. 1. Total ion current chromatogram of raw tholins pyrolysed at 575°C. Labelled species are volatilized aromatic nitrile, unfused and fused aromatic hydrocarbons.

On discarding O from the mass balance the stoichiometry calculated was $C_{11}H_{11}N_2$ (McKay 1996).

Py–GC–MS

Approximately 1 mg of raw tholins with 100 mg of pure SiO_2 was crushed to powder. The powdered mixture was loaded on a platinum filament of the Pyrola® 2000 pyrolyser system. Small and approximately equal quantities of raw tholins samples were pyrolysed at several temperatures – 175, 275, 375, 475 and 575°C – consecutively. The filament was heated up to the set pyrolysis temperature for 2 s. The volatilized species were analysed using a Varian 3800 GC (Varian, Inc.) equipped with a Restek® Rtx-20 chromatographic column (30 m × 0.25 mm × 0.15 μm) and coupled to a Varian 4000 ion-trap MS (Varian, Inc.) with internal ionization. The column temperature was ramped up from 30°C at a rate of 15°C min^{-1} to reach to 250°C where it was maintained constant during the remainder GC run. The total duration of the GC run was 25 min. Further the chemical species separated by the GC were identified by the MS using the scan detection mode at a rate of 1.5 scans s^{-1} and detection range of *m*/*z* 35–1000.

LD–TOF–MS

Raw tholin powder was directly pressed onto a customized removable sample stub that was analysed by LD–TOF–MS (Bruker autoflex™ speed, Bruker Daltonics). Furthermore, 5 mg of raw tholin powder was dissolved in 100 μl *n*-hexane, of which ~ 3 μl *n*-hexane-extracted solution was pipetted onto a highly polished stainless steel multi-target plate for mass analysis. The LD–TOF–MS instrument was equipped with a frequency-tripled Nd:YAG (355 nm) commercial laser running at 50 Hz, with an energy around 200–250 μJ, a pulse width of ~ 3 ns, and laser beam size of $\sim 200 \times 200$ μm^2. A sum of 1500 laser shots (spectra) was collected with the laser rastering over the sample surface. Both positive and negative ion modes were available on this instrument. The tholins

https://doi.org/10.1017/S1473550415000439 Published online by Cambridge University Press

Table 1. *Aromatic hydrocarbons detected in raw tholins using Py–GC–MS.*

Aromatic hydrocarbons	Number of rings	Retention time (min)	SNR (peak-to-peak)	Mass fragments identified
Benzene	1	2.51	6	**78**, 77, 63, 51, 39
Toluene	1	3.37	27	92, **91**, 65, 51, 39
Benzonitrile	1	6.22	32	104, **103**, 76, 75, 50
Ethylbenzene	1	4.34	14	91, **106**, 77, 65, 51
1-ethyl-3-methylbenzene	1	5.42	11	**120**, 105, 91, 77, 65
Naphthalene	2	8.24	12	**128**, 102, 77, 64, 51
Naphthalene-2-carbonitrile	2	11.47	14	**153**, 126, 87, 63, 51
Phenanthrene	3	13.73	11	**178**, 152, 126, 89, 76
6H-cyclobuta[*j, k*]phenanthrene	3	14.81	3	191, 190, **189**, 149, 95

SNR, signal-to-noise ratio.
Bold values signifies Molecular ion peaks.

caused a strong background signal in the positive mode measurements. However, in the negative mode the results showed more identifiable peaks. Therefore, only the negative ion mode data were considered in this work.

Raman spectroscopy

The instrument used was a LabRAM-HR 800 UV Raman spectrometer (Horiba Jobin–Yvon) attached to an Olympus BX41 microscope equipped with an Olympus MPlane 100× objective.

The Raman spectrometer was equipped with a 488 nm-line Ar+ laser (106020B0S, Melles Griot, Carlsbad, CA, USA), with a laser power of 20 mW and a focal length of 800 mm. The laser was dispersed by a 600 litres mm^{-1} grating on a charge-coupled device detector with 1024 × 256 pixels, producing a spectral resolution of 0.43 cm^{-1}. For internal calibration a silicon standard with a major peak at 520.4 cm^{-1} was used. The spectra recording and processing were done with the LabSpec™ version 5.19.17 (Horiba Jobin–Yvon, Villeneuve d'Ascq, France). Background subtraction was applied using manual line fitting. Band fitting for the two main bands was conducted with a Gauss–Lorentz function from the background-corrected spectrum.

FE-SEM

The FE-SEM used was a LEO 1530 Gemini (Carl Zeiss) instrument with an accelerating voltage of 15 kV. The raw tholins samples were mounted on carbon pads and then coated with 15 nm thickness of Pt/Au with a sputter coater. No wet brush was used; the resultant dust was removed with air.

Results and discussion

Py–GC–MS analyses

The tholins pyrolysate chromatogram at 575°C displays aromatic hydrocarbons (Fig. 1) that were identified by linear ion-trap MS based on their fragmentation pattern. Of the numerous chromatograms obtained at different pyrolysis temperatures, the chromatogram at 575 °C, owing to higher temperature, showed the highest diversity of polycyclic aromatic hydrocarbons (PAHs). Therefore, we will only discuss this chromatogram in the following. The GC separated a

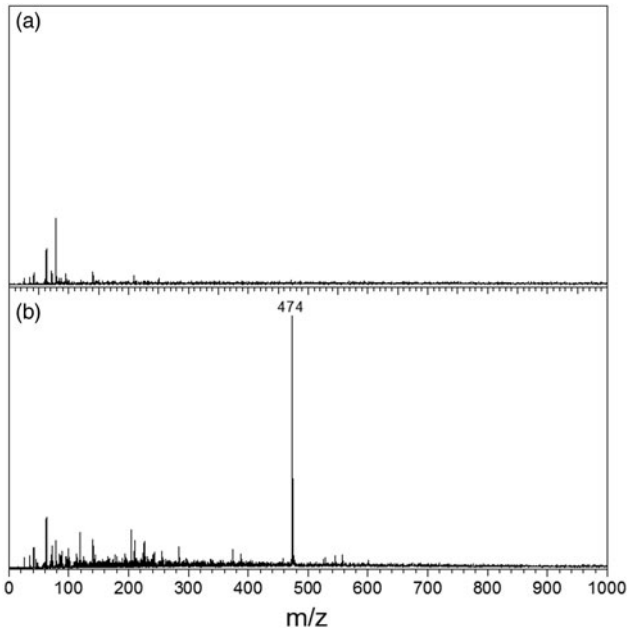


Fig. 2. Negative ion LD–TOF mass spectra of (a) pure *n*-hexane (solvent blank) and (b) *n*-hexane-extracted tholins.

variety of nitrile species that are typical of Titan tholins pyrolysate such as 2-butenenitrile (McGuigan *et al.* 2006), benzonitrile (Coll *et al.* 1998; McGuigan *et al.* 2006; Kawai *et al.* 2013) and 2-napthalenecarbonitrile (Sagan *et al.* 1993). We identified several aromatic hydrocarbons with unfused and fused rings (see Fig. 1 and Table 1).

Imanaka *et al.* (2004) pointed out the PAH abundance in certain types of tholins (Khare *et al.* 1984; Sagan *et al.* 1993; Ehrenfreund *et al.* 1995), whereas deficiency in other types were reported (Coll *et al.* 1999). PAH-abundant Titan tholins were consistently produced in reactors with low pressures (13–26 Pa), relatively high CH_4 concentration (>1%), and with tesla- and inductively coupled cold plasma discharges (Hodyss *et al.* 2004; Trainer *et al.* 2004; Cable *et al.* 2011). In contrast, PAH-deficient Titan tholins have been characteristically produced in reactors maintained at high pressures (~100 Pa), low temperatures (100–150 K) and with capacitively coupled cold plasma discharge (Ramírez *et al.* 2005; Quirico *et al.* 2008).

https://doi.org/10.1017/S1473550415000439 Published online by Cambridge University Press

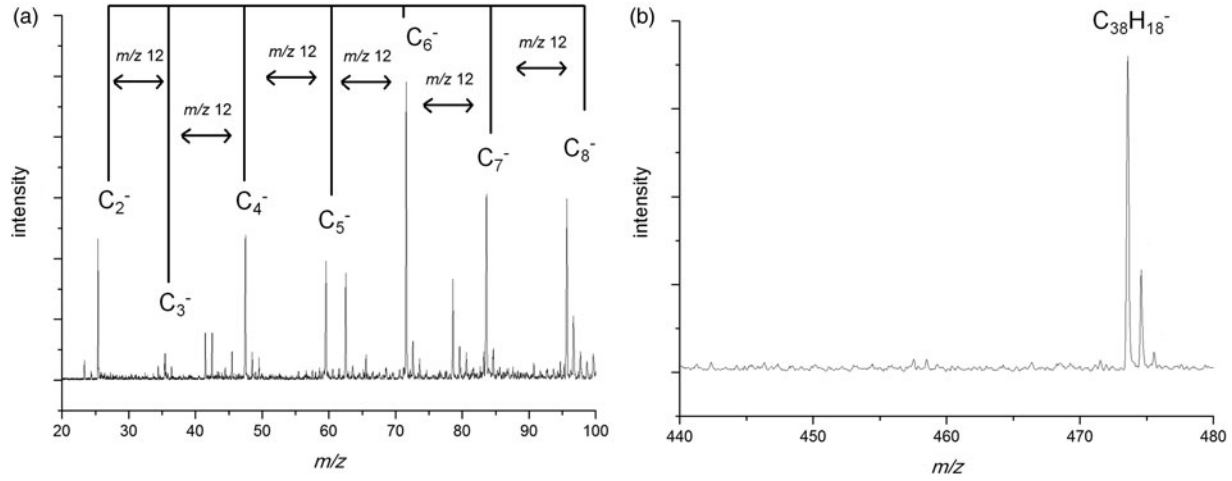


Fig. 3. Negative ion LD–TOF mass spectra of raw tholins at lower *m*/*z* range. (a) Clusters of regularly spaced mass peaks (Δ*m*/*z* 12) in the *m*/*z* range of 20–100. (b) Intense peak at *m*/*z* 474 that could be tentatively assigned to $C_{38}H_{18}^-$.

The tholins in this study were produced at low pressure, with tesla discharge, and with continuous gas flow and high CH_4 content in the starting mixture. These conditions have been shown to correlate with high PAH production (Trainer *et al.* 2004; Cable *et al.* 2011). Trainer *et al.* (2004) reported that particles produced from a mixture of 10% CH_4 in N_2 are consistent with a large fraction of aromatics, including specific *m*/*z* peaks likely due to PAHs. However, at lower concentrations of CH_4 (<1%), the mass fraction of PAHs greatly diminishes and an aliphatic chemical formation pathway dominates. Benzene (C_6H_6) and toluene ($C_6H_5CH_3$) identified in the pyrolysate are known precursors of PAHs, and their detection among the other volatilized PAHs direct that they were volatilized from a large PAH (LPAH) structural component existing within the greater chemical structure of tholins.

LD–TOF–MS analyses

We obtained mass spectra of both raw and *n*-hexane extracted tholins, and the latter was used as a blank measurement. The spectrum of *n*-hexane-extracted tholins was also compared with that of pure *n*-hexane which was used as solvent blank reference (Fig. 2). The comparison clearly distinguishes the mass peaks contributed by the organic solvent *n*-hexane (Fig. 2(a)) with those contributed by tholins (Fig. 2(b)).

Figure 3 shows two individual *m*/*z* spectral segments of negative ion mode measurements of *n*-hexane-extracted tholins. The segment from *m*/*z* 20–100 of *n*-hexane-extracted tholins (Fig. 3(a)) displays regularly spaced peak clusters, each separated by Δ *m*/*z* 12 corresponding to the mass of atomic carbon. The clusters were observed from *m*/*z* 24 to 96 and could be assigned to negatively ionized C_2 to C_8. Although the structural conformations and the formation mechanisms of the assigned species could not be construed, we postulate these peaks arise due to carbon vapours formed from LD of a highly carbonaceous tholins. Many ion species that we tentatively assigned to the observed peaks are known precursors to soot (Cochran 1987; Gerhardt *et al.* 1987; Ebert 1990; Gingerich *et al.* 1994) and mass spectrometric studies have already demonstrated emission of negative ionized C_2 to C_8 on molecular sublimation of graphite (Honig 1954). The species that could represent these peaks have also been observed astronomically. Diatomic carbon (C_2) was detected in the jets of comet C/1989 X1 (Austin) (Suzuki *et al.* 1990); triatomic carbon (C_3) was detected in comets and circumstellar discs (Douglas 1951; Goebel *et al.* 1978; Cernicharo *et al.* 2000; Haddad *et al.* 2013). Linear C_4 was first identified and characterized in gas phase, when it was produced by ultraviolet laser vaporization of graphite (Heath & Saykally 1991). Both C_4 and C_5 are speculated in carbon-rich evolved stars (IRC+10216) and in the molecular cloud Sagittarius B2 (Bernath *et al.* 1989; Cernicharo *et al.* 2002). We also observed a strong peak at *m*/*z* 63 that could be tentatively assigned to $C_5H_3^-$. $C_5H_3^-$ is an anticipated species in interstellar clouds (Herbst & Leung 1989) and acts as a precursor to fullerenes, PAH and soot (Bettens & Herbst 1997; Richter & Howard 2000; Hansen *et al.* 2006).

In the next segment of the *n*-hexane-extracted tholins mass spectrum (Fig. 3(b)) we observed a cluster with a strong peak at *m*/*z* 474 and minor peaks at 475 and 476. With confirmed reproducibility of these peaks, we speculate that the strongest peak (*m*/*z* 474) may be a potential LPAH with a tentative molecular formula $C_{38}H_{18}^-$. Semi-empirical studies state that $C_{38}H_{18}^-$ is a conformationally stable LPAH (Pogodin & Agranat 2001) and has also been detected in high resolution mass spectral studies of coke synthesized from pyrolysis of benzene (Kousoku *et al.* 2014). However, we were unable to comprehend the reason for the resolution of this peak cluster and the absence of other nearby peaks with comparable intensities.

Figure 4 shows two individual *m*/*z* spectral segments of negative ion mode measurements of raw tholins along with the entire spectrum (Fig. 4(c)). In the raw tholins mass spectrum (Fig. 4(a)) we observed peaks at *m*/*z* 696, 708, 924 and 936, which could be tentatively estimated for C_{58}^-, C_{59}^-, C_{77}^-

https://doi.org/10.1017/S1473550415000439 Published online by Cambridge University Press

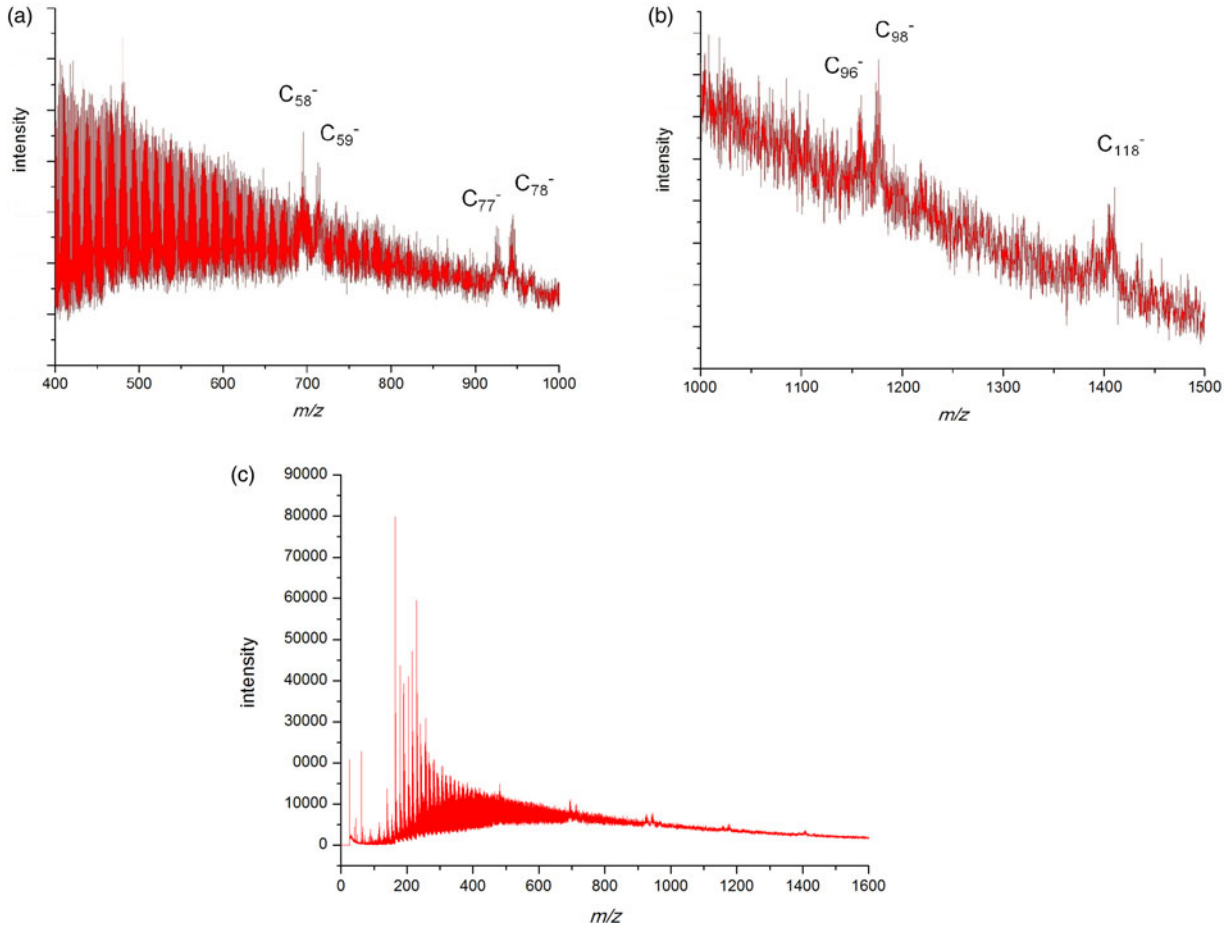


Fig. 4. Negative ion LD–TOF mass spectra of raw tholins at higher *m*/*z* range. (a) Segment of spectrum displaying mass peak clusters at around *m*/*z* 696, 708, 924 and 936 that could be tentatively assigned to C_{58}^-, C_{59}^-, C_{77}^- and C_{78}^-, respectively. (b) Segment displaying peak clusters at *m*/*z* 1153, 1177 and 1417 that could be tentatively assigned to C_{96}^-, C_{98}^- and C_{118}^-, respectively. (c) Entire mass spectrum of raw tholins including the segments (a) and (b).

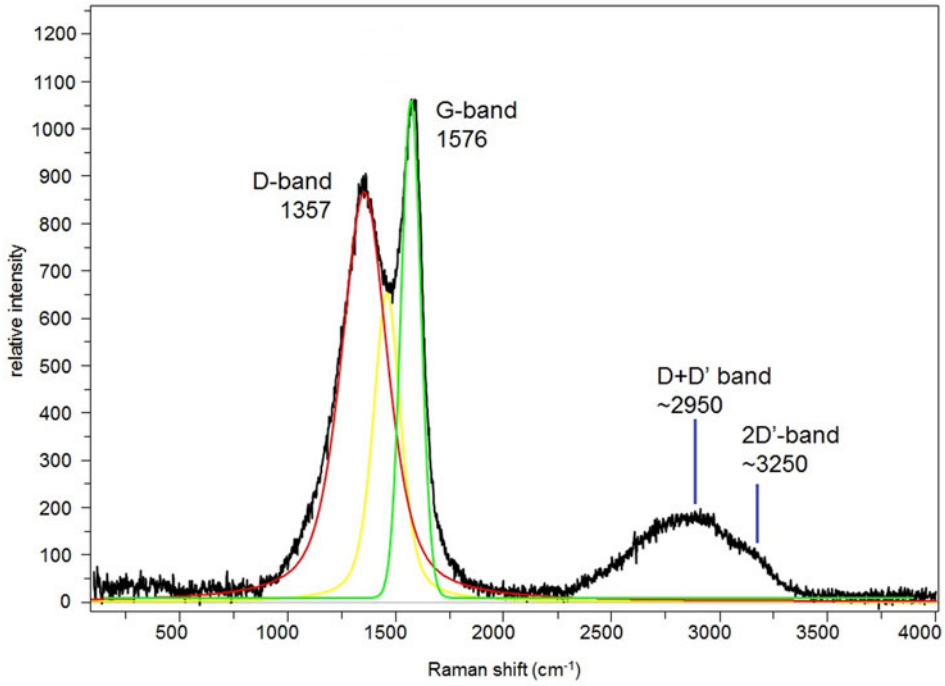


Fig. 5. Raman spectrum (λ 488 nm) decomposition into three Gaussian curves (coloured red, yellow and green) for raw tholins.

https://doi.org/10.1017/S1473550415000439 Published online by Cambridge University Press

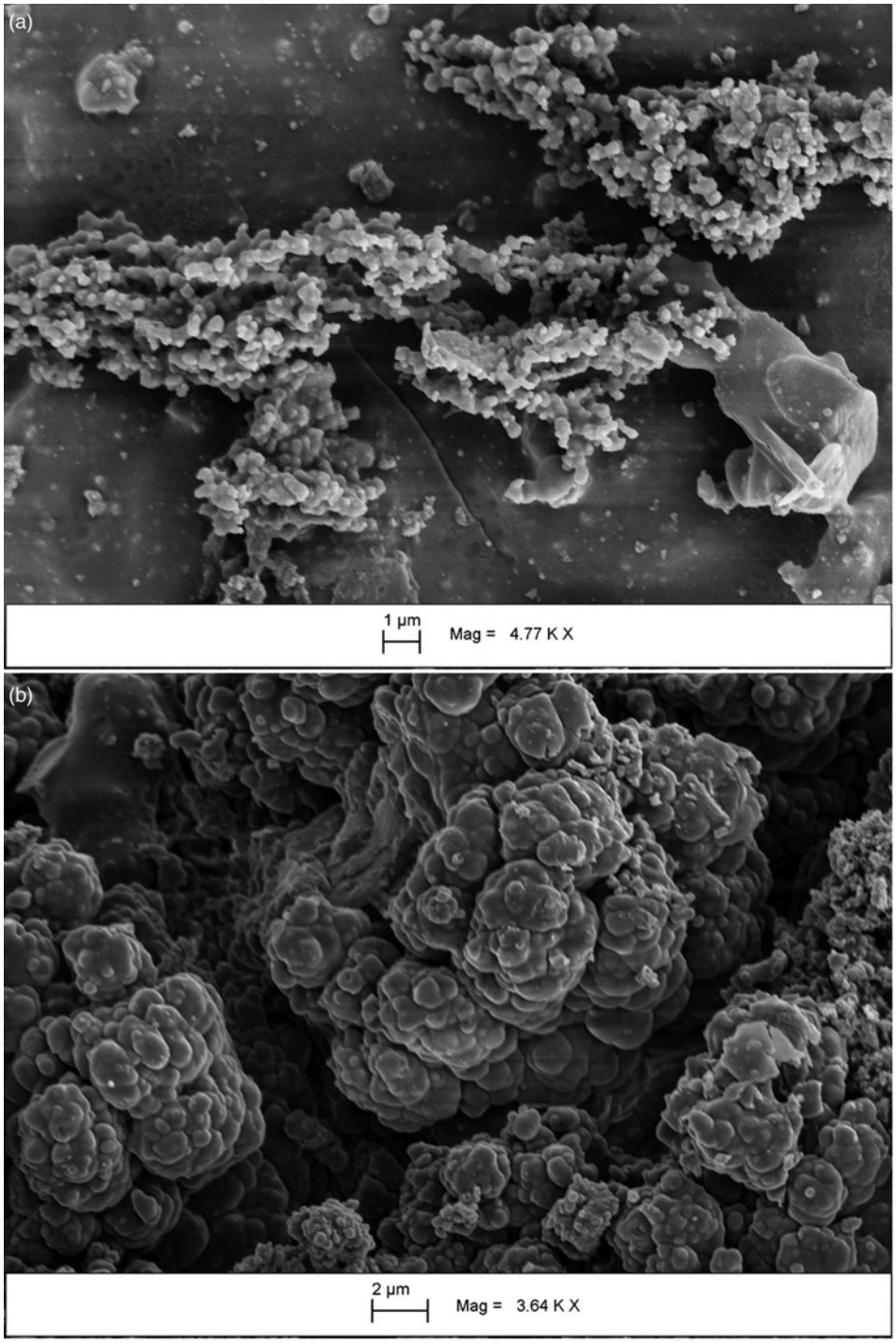


Fig. 6. High-resolution FE-SEM images of raw tholins displaying two distinct carbonaceous structures: (a) fractal-like soot particle aggregates and (b) cauliflower-like graphitic globules.

and C_{78}^{-}, respectively. Furthermore, in the next segment of the same mass spectrum (Fig. 4(b)) mass peaks at *m*/*z* 1153, 1177 and 1417 could be tentatively estimated as average molecular masses for C_{96}^{-}, C_{98}^{-} and C_{118}^{-}, respectively.

Raman spectroscopy analyses

The variations in the carbonaceous structure of tholins were studied using Raman spectroscopy. The Raman spectrum revealed two prominent features, the D band at 1357 cm^{-1} and G band at 1576 cm^{-1} (Fig. 5). These bands are a straightforward characteristic of disordered or defected graphitic material (Vidano & Fischbach 1978). The D band has an A_{1g} symmetry in first-order scattering progression that arises due to defects in the sp^2 bonded carbon graphite structure (Ferrari & Robertson 2000). These defects are probably due to in plane substituted H and N heteroatoms and vacancies

https://doi.org/10.1017/S1473550415000439 Published online by Cambridge University Press

(Gupta & Saxena 2009) within the tholins. The G band is due to tangential stretching of C–C bonds having an E_{2g} symmetry.

The $A_{g(2)}$ symmetry at around 1462 cm^{-1}, known to be the most prominent Raman feature exhibited by C_{60} fullerene (Gupta & Saxena 2009) is not clearly visible in our Raman spectrum (Fig. 5). Also, the LD–TOF–MS did not reveal a mass peak at *m*/*z* 720 that could be assigned to C_{60} (Fig. 4 (a)). The peak at $\sim$2950 cm^{-1} is identified as the D + D′ band. The broad shape of this peak is characteristic for defected graphite structures (Nemanich & Solin 1977; Sato *et al.* 1978).

The D + D′ band displays a shouldered peak at $\sim$3250 cm^{-1}, characteristic to ordered graphite (Nemanich & Solin 1977; Sato *et al.* 1978) identified as 2D′ band. Taken together, the D + D′ and 2D′ bands suggest that the tholins structure probably consists of both disordered and ordered graphite.

FE-SEM analyses

The FE-SEM images (Fig. 6) of raw tholins display two distinct carbonaceous structures – fractal-like aggregates of soot nanoparticles (Fig. 6(a)) and cauliflower-type graphitic globules (Fig. 6(b)). The nanoparticles monomers do not appear to be uniform in size; the largest are $\sim$100 nm in diameter and they appear to be growing in a three-dimensional fractal manner forming aggregates. The loosely packed cauliflower-type graphitic globules have non-uniform diameters ranging from 100 to 1000 nm. These globules appear concentric and discontinuous; the latter probably indicating diversity in the structural conformations of the nucleation centres. Both the aggregates and the globules were possibly formed from different precursor LPAHs and with different fullerenes acting as nucleation centre. But, the exact synthesis mechanism of carbonized material from LPAHs is yet to be understood.

Our observations from various analytical techniques now enable us to conceive a 'proof of concept' that N_2:CH_4 (9:1) gaseous mixture, when subjected to tesla coil discharge, forms extensive PAH assemblages and, with longer duration of irradiation, eventually undergoes carbonization. The presence of H and N heteroatoms in the starting mixture and the oxidation contributed O atoms should be potentially forming defects in the graphite. However, certain segments of tholins have seemingly formed ordered graphite, indicating complete elimination of heteroatoms. The regularly spaced mass peaks from *m*/*z* 24 to 96 and the mass peak clusters observed at higher *m*/*z* hint at the presence of graphitic structure. LD of graphite is known to generate fullerenes and so the identification of native fullerenes within graphitic material by LD–TOF–MS have for long been argued (Kroto *et al.* 1985; Hammond & Zare 2008).

In this study, however, we did not intend to determine the nativity of fullerenes within tholins. The occurrence of high molecular mass peaks in our LD–TOF–MS data (Fig. 4), which could be tentatively assigned to fullerenes, directs to the existence of graphite components within the larger tholins structure. Since we were unable to identify any Raman signatures indicative for fullerenes, we preliminarily infer that the tholins apparently do not contain innate fullerenes. Nevertheless, we do not completely rule out the possible role of 'curved' fullerenes as an intermediate transition structure between the 'planar' LPAH and 'curved' primary soot particles, the latter being observed in the FE-SEM. This assumption stands on a well-established research that PAHs contribute to the generation of soot (Faccinetto *et al.* 2011). Therefore, we stress on the need for further research in exploring the characteristics of any tholins innate fullerenes.

Carbonaceous material exhibits a variety of chemical bond hybridizations (*sp, sp*^{2} and *sp*^{3}) that in turn cause characteristic optical features. In graphite, the C–C bonds are trigonal, *sp*^{2} hybridized and form extensive planar structures with sixfold rings. The planar structure leads to complete π-electron delocalization thereby imparting the low albedo. The N heteroatom in disordered graphite of tholins could further assist the π-electron delocalization due to its lone pair of electrons (Cruikshank *et al.* 2005). The low geometric albedo of comets and other similar SSSBs could possibly be arising from graphitization of tholin-like complex organic material present on their surfaces.

The potential presence of graphitic tholins-like material on Centaurs, TNOs and comets is of great astrobiological significance. Such material possibly could have comprised a large fraction of the organic payload of the $\sim 1.8 \times 10^{23}$ g of cometary material delivered during the late heavy bombardment ($\sim$4.1–3.8 Ga) to the primitive Earth (Gomes *et al.* 2005). Tholin-like material could be a candidate source of prebiotic amino acids (Khare *et al.* 1986) and graphite; the latter probably acting as a template for the synthesis of a primordial genetic architecture (Sowerby *et al.* 2001).

Conclusions

In astronomical models of several Centaurs and TNOs, Titan tholins were presumed to simulate only the NIR signature while amorphous carbon within the same mixtures was assumed to simulate the low albedo. Based on our observations on Titan tholins, we postulate that the low geometric albedo must not necessarily be due to a separate source of amorphous carbon. Alternatively, it can also result from the gradual carbonization of the same complex organic material that contributes to the NIR signature. Although Titan tholins may not be entirely representative of organic material on Centaurs and TNOs, the overarching common properties of complex organic materials makes them close analogues. Therefore, the structural and chemical properties of complex organic materials on Centaurs and TNOs have to be further explored.

Acknowledgements

This paper is dedicated to the late Dr Bishun Khare, who passed away on August 20, 2013. Khare made noteworthy contribution to the global effort to understand tholins and encouraged initiating this study as well. We thank Dr Hiroshi Imanaka, David Beeler and Dr Seema Jagota for discussion of tholins plasma-discharge experimental setup. We thank Dr Martin Hilchenbach for the

https://doi.org/10.1017/S1473550415000439 Published online by Cambridge University Press

discussions on preliminary Raman analyses of tholins. C. G. acknowledges the International Max Planck Research School for the Doctoral and Postdoctoral Fellowships awarded by the Max Planck Institute for Solar System Research, Germany. T.G. was supported by an appointment to the NASA Postdoctoral Programme at the Goddard Space Flight Center, administered by Oak Ridge Associated Universities through a contract with NASA. The authors would like to thank the reviewers, Dr Rainer Oswald and Dr Tim Leefmann for their valuable remarks and suggestions to improve this paper.

References

Bandurski, E.L. & Nagy, B. (1976). *Geochim. Cosmochim. Acta* **40**, 1397–1406.

Barucci, M.A., de Bergh, C., Cuby, J.-G., Le Bras, A., Schmitt, B. & Romon, J. (2000). *Astron. Astrophys.* **357**, 53–56.

Bernath, P.F., Hinkle, K.H. & Keady, J.J. (1989). *Science* **244**, 562–564.

Bettens, R.P.A. & Herbst, E. (1997). *Astrophys. J.* **478**, 585–593.

Cable, M.L., Hörst, S.M., Hodyss, R., Beauchamp, P.M., Smith, M.A. & Willis, P.A. (2011). *Chem. Rev.* **112**, 1882–1909.

Cernicharo, J., Goicoechea, J.R. & Caux, E. (2000). *Astrophys. J.* **534**, 199–202.

Cernicharo, J., Goicoechea, J.R. & Benilan, Y. (2002). *Astrophys. J.* **580**, 157–160.

Cochran, A.L. (1987). *Astron. J.* **92**, 231–238.

Coll, P., Coscia, D., Gazeau, M.-C., Guez, L. & Raulin, F. (1998). *Orig. Life Evol. Biosph.* **28**, 195–213.

Coll, P., Coscia, D., Smith, N., Gazeau, M-C., Ramírez, S.I., Cernogara, G., Israël, G. & Raulin, F. (1999). *Planet. Space Sci.* **47**, 1331–1340.

Cruikshank, D. (1987). *Adv. Space Res.* **7**, 109–120.

Cruikshank, D.P. *et al.* (1998). *Icarus* **135**, 389–407.

Cruikshank, D.P., Imanaka, H. & Dalle Ore, C.M. (2005). *Adv. Space Res.* **36**, 178–183.

DeMeo, F.E., Barucci, M.A., Merlin, F., Guilbert-Lepoutre, A., Alvarez-Candal, A., Delsanti, A., Fornasier, S. & de Bergh, C. (2010). *Astron. Astrophys.* **521**, A35.

Dorresoundiram, A., Barucci, M.A., Tozzi, G.P., Poulet, F., Boehnhardt, H., de Bergh, C. & Peixinho, N. (2005). *Planet. Space Sci.* **53**, 1501–1509.

Dotto, E., Barucci, M.A., Leyrat, C., Romon, J., de Bergh, C. & Licandro, J. (2003a). *Icarus* **164**, 122–126.

Dotto, E., Barucci, M.A., Boehnhardt, H., Romon, J., Dorresoundiram, A., Peixinho, N., de Bergh, C. & Lazzarin, M. (2003b). *Icarus* **162**, 408–414.

Douglas, A.E. (1951). *Astrophys. J.* **114**, 466–468.

Ebert, L.B. (1990). *Science* **247**, 1468–1471.

Ehrenfreund, P., Boon, J.J., Commandeur, J., Sagan, C., Thompson, W.R. & Khare, B.N. (1995). *Adv. Space Res.* **15**, 335–342.

Faccinetto, A., Desgroux, P., Ziskind, M., Therssen, E. & Focsa, C. (2011). *Combust. Flame* **158**, 227–239.

Ferrari, A.C. & Robertson, J. (2000). *Phys. Rev. B* **61**, 95–107.

Gerhardt, Ph., Löffler, S. & Homann, K.H. (1987). *Chem. Phys. Lett.* **137**, 306–310.

Gingerich, K.A., Finkbeiner, H.C. & Schmude, R.W. Jr. (1994). *J. Am. Chem. Soc.* **116**, 3884–3888.

Goebel, J.H., Bregman, J.D., Strecker, D.W., Witteborn, F.C. & Erickson, E. F. (1978). *Astrophys. J.* **222**, 129–132.

Gomes, R., Levison, H.F., Tsiganis, K. & Morbidelli, A. (2005). *Nature* **435**, 466–469.

Gradie, J. & Veverka, J. (1980). *Nature* **283**, 840–841.

Gupta, S. & Saxena, A. (2009). *J. Raman Spectrosc.* **40**, 1127–1137.

Haddad, M.A., Zhao, D., Linnartz, H. & Ubachs, W. (2013). *Proc. Int. Astron. Union* **9**, 297–299.

Hammond, M.R. & Zare, R.N. (2008). *Geochim. Cosmochim. Acta* **72**, 5521–5529.

Hansen, N., Klippenstein, S.J., Miller, J.A., Wang, J., Cool, T.A., Law, M.E., Westmoreland, P.R., Kasper, T. & Höinghaus, K.K. (2006). *J. Phys. Chem. A* **110**, 4376–4388.

Hayatsu, R. & Anders, E. (1981). *Top. Curr. Chem.* **99**, 1–37.

Hayatsu, R., Studier, M.H. & Anders, E. (1971). *Geochim. Cosmochim. Acta* **35**, 939–951.

Heath, J.R. & Saykally, R.J. (1991). *J. Chem. Phys.* **94**, 3271–3273.

Herbst, E. & Leung, C.M. (1989). *Astrophys. J.* **69**, 271–300.

Hodyss, R., McDonald, G.D., Sarker, N., Smith, M.A., Beauchamp, P.A. & Beauchamp, J.L. (2004). *Icarus* **171**, 525–530.

Honig, R.E. (1954). *J. Chem. Phys.* **22**, 126–131.

Imanaka, H., Khare, B.N., Elsila, J.E., Bakes, E.L.O., McKay, C.P., Cruikshank, D.P., Sugita, S., Matsui, T. & Zare, R.N. (2004). *Icarus* **168**, 344–366.

Kawai, J., Jagota, S., Kaneko, T., Obayashi, Y., Yoshimura, Y., Khare, B. N., Deamer, D.W., McKay, C.P. & Kobayashi, K. (2013). *Int. J. Astrobiol.* **12**, 282–291.

Kerridge, J.F. (1999). *Space Sci. Rev.* **90**, 275–288.

Khare, B.N. *et al.* (1984). *Adv. Space Res.* **4**, 59–68.

Khare, B.N., Sagan, C., Ogino, H., Nagy, B., Er, C., Schram, K.H. & Arakawa, E.T. (1986). *Icarus* **68**, 176–184.

Khare, B.N., Thompson, W.R., Chyba, C.F., Arakawa, E.T. & Sagan, C. (1989). *Adv. Space Res.* **9**, 41–53.

Khare, B.N., Thompson, W.R., Cheng, L., Chyba, C., Sagan, C., Arakawa, E.T., Meisse, C. & Tuminello, P.S. (1993). *Icarus* **103**, 290–300.

Kousoku, A., Ashida, R., Miyasato, A., Miyake, M. & Miura, K. (2014). *Proc. of the 24th Saudi–Japan Annual Symp. Catalysts in Petroleum Refining & Petrochemicals, KFUPM*, Dhahran, Saudi Arabia, 1–2 December, 2014.

Kroto, H.W., Heath, J.R., O'Brien, S.C., Curl, R.F. & Smalley, R.E. (1985). *Nature* **318**, 162–163.

Kwok, S. (2009). *Astrophys. Space Sci.* **319**, 5–21.

McDonald, G.D., Thompson, W.R., Heinrich, M., Khare, B.N. & Sagan, C. (1994). *Icarus* **108**, 137–145.

McDonald, G.D., Whited, L.D., DeRuiter, C., Khare, B.N., Patnaik, A. & Sagan, C. (1996). *Icarus* **122**, 107–117.

McGuigan, M., Waite, J.H., Imanaka, H. & Sacks, R.D. (2006). *J. Chromatogr. A* **1132**, 280–288.

McKay, C.P. (1996). *Planet. Space Sci.* **44**, 741–747.

Nemanich, R.J. & Solin, S.A. (1977). *Solid State Commun.* **23**, 417–420.

Pogodin, S. & Agranat, I. (2001). *Polycyl. Aromat. Compd.* **18**, 247–263.

Quirico, E. *et al.* (2008). *Icarus* **198**, 218–231.

Ramírez, S.I., Navarro-González, R., Coll, P. & Raulin, F. (2005). *Adv. Space Res.* **36**, 274–280.

Richter, H. & Howard, J.B. (2000). *Prog. Energy Combust. Sci.* **26**, 565–608.

Sagan, C. & Khare, B.N. (1979). *Nature* **277**, 102–107.

Sagan, C., Khare, B.N., Thompson, W.R., McDonald, G.D., Wing, M.R., Bada, J.L., Vo-Dinh, T. & Arakawa, E.T. (1993). *Astrophys. J.* **414**, 399–405.

Sato, Y., Kamo, M. & Setaka, N. (1978). *Carbon* **16**, 279–280.

Sowerby, S.J., Cohn, C.A., Heckl, W.M. & Holm, N.G. (2001). *Proc. Natl. Acad. Sci. USA* **98**, 820–822.

Studier, M.H., Hayatsu, R. & Anders, E. (1972). *Geochim. Cosmochim. Acta* **36**, 189–215.

Suzuki, B., Kurihara, H. & Watanabe, J. (1990). *Publ. Astron. Soc. Japan* **42**, 93–97.

Trainer, M.G., Pavlov, A.A., Jimenez, J.L., McKay, C.P., Worsnop, D.R., Toon, O.B. & Tolbert, M.A. (2004). *Geophys. Res. Lett.* **31**, L17S08, doi: 10.1029/2004GL019859.

Vidano, R. & Fischbach, D.B. (1978). *J. Am. Ceram. Soc.* **61**, 13–17.

https://doi.org/10.1017/S1473550415000439 Published online by Cambridge University Press